Cu NMR and NQR in High T_c Oxides $YBa_2Cu_3O_x$ ($6.0 \leq x \leq 6.98$) and Related Material CuO †

T. Shimizu, H. Yasuoka, T. Tsuda , K. Koga and Y. Ueda

Institute for Solid State Physics, University of Tokyo
7-22-1 Roppongi, Minato-ku, Tokyo 106, Japan

ABSTRACT: ^{63}Cu Knight shift measurements have been made in the normal state of superconductors $YBa_2Cu_3O_x$ ($x = 6.48$ and 6.98) and in the paramagnetic state of the related material CuO. The $K - \chi$ plot analysis has been made, for the first time, for the Cu NMR in the high T_c oxide and CuO. The results show quite characteristic features of the local electronic states of the substances. In $YBa_2Cu_3O_x$ system, Cu(2) plain sites persist in a divalent charged state between $6.0 \leq x \leq 6.98$, while Cu(1) chain sites exhibit a mixed valence in space depending on the oxygen coordination number. It is also found, from a detailed analysis of the hyperfine field (hf), that a usual ionic model of a Cu^{2+} ion in a tetragonal field can be primarily used to describe the wave function of magnetic electrons of Cu^{2+} ions in both CuO and $YBa_2Cu_3O_x$. We found, however, only in $YBa_2Cu_3O_x$ system an additional and anomalous contribution to the Fermi contact hf, which is a large and positive hf more than 100 kOe/μ_B. Such an anomalous hf has never been found in transition metal compounds before, therefore characterizing an outstanding electronic feature of high T_c copper oxide system. It should be stressed that the origin of this anomalous hf can not be attributed to the extra holes, because there exists approximately the same amount of the anomalous hf even in the insulating phase ($x = 6.0$). Among several possible mechanisms to account for the anomalous hf, the dominant mechanism in the present case is most likely the supertransferred hyperfine interaction arising from a covalent electron transfer through the linear bonds Cu^{2+}—O^{2-}—Cu^{2+}. From the viewpoint of structural consideration, this mechanism is considered to be favored in the perovskite type structure *i.e.*, a corner-sharing net-work in a [$-CuO_2-$] sheet, but not favored in a type of edge-sharing net-work appearing in CuO. From the viewpoint of energetics, the present results reflects the small value of the charge transfer gap (Δ) in $YBa_2Cu_3O_x$ system.

§1.Introduction

The epoch-making discovery of high temperature superconductivity in copper oxides (Bednorz and Müller, 1986) is followed by considerable efforts to understand the electronic states underlying the superconductivity. The common physical constitution of these materials *i.e.*, oxides of copper and layered perovskite structure (see, as a review article, Pickett, 1989), implies that an appropriate understand of electronic structure is a key point. A general feature of the electronic state can be seen in the phase diagram for $YBa_2Cu_3O_x$ system (Tranquada *et al.*, 1988 and Cava *et al.*, 1988), as shown in Fig.1. When the oxide is stoichiometric ($x = 6.0$), the electronic state is a Mott-Hubbard insulator and antiferromagnet. When additional oxygens are introduced in the system, an insulator to superconductor transition occurs around about $x = 6.3$. A fundamental problem of the high T_c superconductors is how to describe the electronic state in such a highly correlated electron system and to relate it with a mechanism of the superconductivity.

The nuclear magnetic resonance (NMR) and nuclear quadrupole resonance (NQR) have been powerful techniques to elucidate the local electronic state in materials. In this paper we present our recent results about spectral investigation of Cu NMR and NQR in $YBa_2Cu_3O_x$ system and the related material CuO, putting special emphasis on a difference in the underlying electronic state between the two copper oxide systems.

It is also seen in Fig.1 that the superconducting phase has two plateaus of T_c, *i.e.*, 90 K for oxygen rich phase and 60 K for the intermediate concentration of oxygen. These two superconducting phases can be distinguished also from the crystallographic point of view. In the $x = 7.0$ phase, four oxygen sites located around Cu(1) chain sites are fully occupied, as seen in

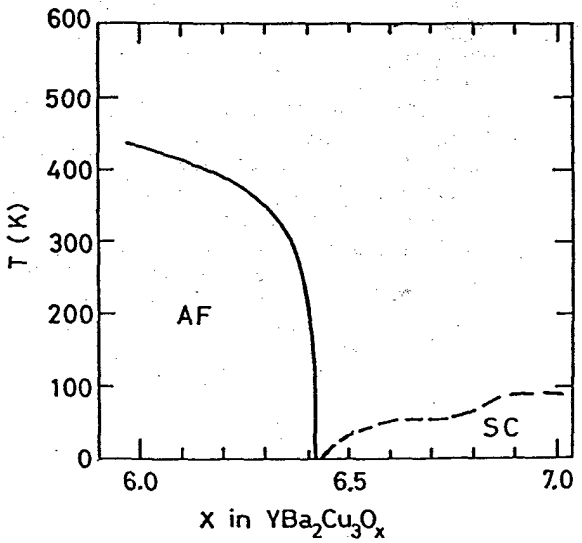

Fig.1. A phase diagram showing the electronic states of $YBa_2Cu_3O_x$. AF and SC denotes antiferromagnetic and superconducting phase, respectively.

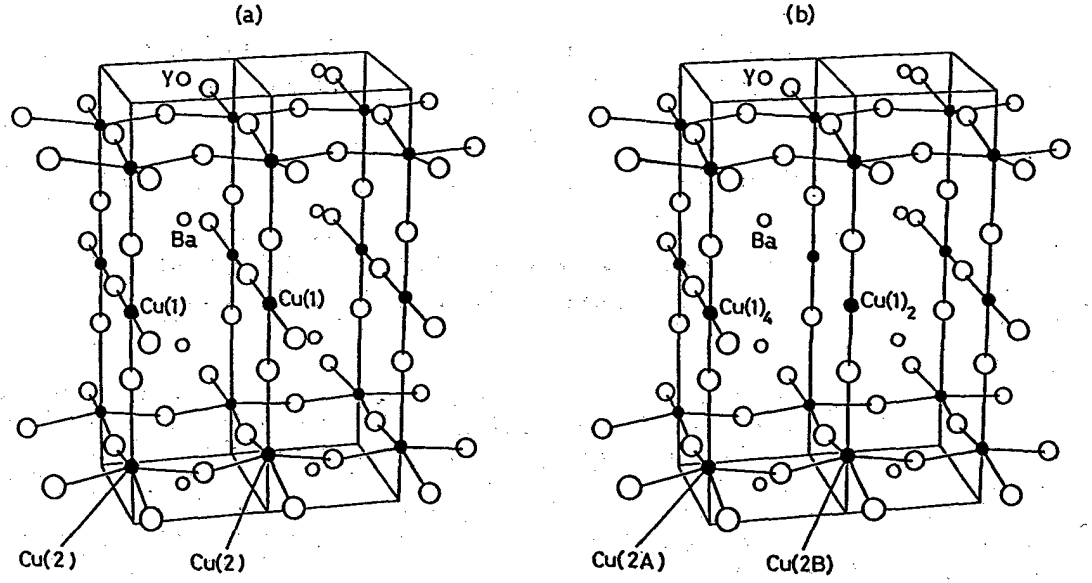

Fig.2. Crystal structures of (a): $YBa_2Cu_3O_{7.0}$ and (b): $YBa_2Cu_3O_{6.5}$.

Fig.2(a). On the other hand, in the $x = 6.5$ phase, if the ideal structure is realized, the half of oxygen atoms in the chains are depleted along the original b-axis, as in Fig.2(b). Thus the unit cell becomes doubled in the direction of original a-axis.

§2. Experimental Procedures

2.1. Sample Preparation

It has been well known that a number of physical quantities of $YBa_2Cu_3O_x$ strongly depends on the preparation procedure owing to the oxygen stoichiometry and order-disorder transition. Although the details have been published elsewhere (Ueda and Kosuge, 1988), we summarized briefly the procedure.

The starting material of $YBa_2Cu_3O_x$ were prepared by solid state reaction of Y_2O_3, $BaCO_3$ and CuO. The mixtures were pelletized, followed by heating up to 900 °C in air, and then ground and reheated. This process was repeated several times, following the final annealing for 5hrs at 500 °C in air. The obtained material was confirmed to be a single phase with orthorhombic $YBa_2Cu_3O_x$. The samples with various oxygen content were prepared from the sintered (at 900 °C) pellets as follows. Each of the pellets was precisely weighted and firstly heated under air at 10 °C/min up to 800 °C and then cooled at the same rate at room temperature. In this run, the trace of the thermogravimetric analysis (TGA) shows a distinct hump in the curvature at 650 °C, corresponding to the orthorhombic to tetragonal phase transition, The composition of the material at the temperature has been well established to be $x = 6.50$ in equilibrium. The pellet was subsequently heated under oxygen or nitrogen (less than 0.001% O_2) gas at 10 °C/min up to the temperature range of 400–700 °C, depending on the aimed value of x, and then cooled slowly at the rata of 2.5 °C/min. to room temperature. The oxygen content of the samples obtained by this treatment was determined by weigh loss or gain, between the weight at 650 °C ($x = 6.50$) and the final point in TGA. The accuracy of the microbalence was ±0.1 mg in weight, corresponding to ±0.21 in x.

2.2. NMR and Magnetic Susceptibility

Both the NMR and NQR experiments were performed by using a coherent type pulsed NMR spectrometer. The NQR spectra were taken by measuring the spin-echo amplitude as a function of the frequency point by point. The NMR spectra were taken by two different methods. The one was a Fourier transform of a spin-echo observed at fixed frequency and field. This technique was available for the case of relatively narrow spectrum with less than 100 Oe at full width of half maximum (FWHM). The other spectrum was taken by a box car integration of the gated spin-echo signal, while sweeping the magnetic field. The applied magnetic field was made by superconducting solenoid up to 83 kOe.

The all samples used in the present study were polycrystals. In order to measure the Knight shift as accurate as possible, we prepared oriented powdered samples for $YBa_2Cu_3O_{6.98}$ and $YBa_2Cu_3O_{6.48}$ with the c-axis well aligned and then obtained sharp NMR lines. Such alignment was easily achieved by exposing the fine powder mixed with epoxy to a magnetic field (about 80 kOe) to, as described by Farrel *et al.* (1987).

The magnetic susceptibility was measured by a Faraday balance magnetic pendulum at a field of 11 kOe and in a temperature range between 4.2 K and 300 K. The measurements was made for polycrystalline sample of 0.5–1.0 g in weight.

§3. Experimental Results for $YBa_2Cu_3O_x$

3.1. Magnetic Susceptibility

Fig.3 shows the temperature dependence of susceptibility for $YBa_2Cu_3O_x$. All points in this figure show raw data without any corrections for spurious Curie-Weiss terms due to some paramagnetic impurity phase, confirming ultra-high quality of our samples.

For $x = 6.98$ sample, the susceptibility shows essentially temperature independent behavior above about 150 K. A careful susceptibility measurement, however, has revealed a steep decrease just above T_c=93 K, as

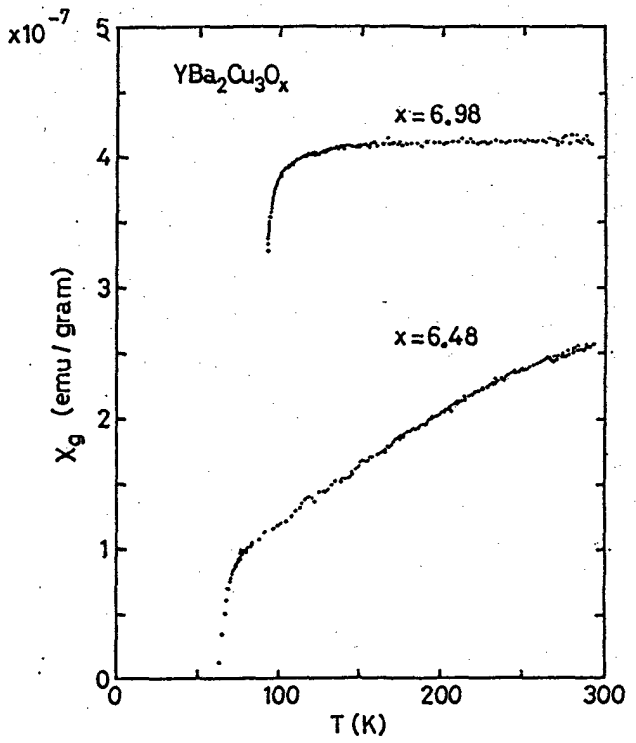

Fig.3. Temperature dependences of susceptibilities of $YBa_2Cu_3O_{6.98}$ and $YBa_2Cu_3O_{6.48}$. The measurement for $YBa_2Cu_3O_{6.98}$ has been performed upon slow cooling, in order to ensure the drastic temperature dependence observed just above $Tc = 93$ K.

can be clearly seen in Fig.3, suggesting an appearance of superconducting fluctuation diamagnetism above T_c. Several authors have already presented analysis and discussions on the susceptibility based on a model of superconducting fluctuation diamagnetism (Kanoda *et al.*, 1988, Kawagoe *et al.*, 1988 and Annet *et al.*, 1988).

For $x = 6.48$ sample the susceptibility is dependent largely on temperature, as shown in Fig.5. This is not due to a superconducting fluctuation diamagnetism. Our sample of $x = 6.48$ shows the bulk superconductivity with $T_c = 60$ K.

3.2. Cu NQR Spectra

Corresponding to the two crystallographic phases shown in Fig.2, distinct line profiles have been obtained in the Cu-NQR spectra for $YBa_2Cu_3O_{6.98}$ and $YBa_2Cu_3O_{6.48}$, as shown in Figs.4(a) and (b), respectively. Site assignments for the NQR lines in the $x = 7.0$ phase have been well established by now; the pair of $^{63}Cu/^{65}Cu$ NQR lines observed at 31.5/29.1 MHz and 22.5/20.8 MHz are assigned to $^{63}Cu(2)$ plane sites and $^{63}Cu(1)$ chain sites, respectively. This site assignment has been achieved by several groups and different methods, including (1) investigation of the symmetry of electric field gradient (EFG) tensors at Cu sites (Shimizu *et al.*, 1988 and Pennington *et al.*, 1988), (2) study of the effect of transferred (predominantly dipole) hyperfine field from localized 4f electrons in magnetic isomorph $RBa_2Cu_3O_7$ where R=Gd (Hammel *et al.*, 1988), Sm and Nd (Kohori *et al.*, 1988), (3) measurement of absolute (Walstedt *et al.*, 1988) or relative (Mali *et al.*, 1987) intensity of each Cu line.

For the $x = 6.5$ phase, there have been few works so far in which site assignments for the whole NQR lines are presented. By an analysis which are described in detailed below, we could have obtained the site assignment for the observed pairs of $^{63}Cu/^{65}Cu$ NQR frequencies as follows; 31.4/29.0 (2-fold Cu(1)), 30.6/28.3 (Cu(2A) neighboring 4-fold Cu(1)), 27.8/25.7 (Cu(2B) neighboring 2-fold Cu(1)), 24.0/22.2 (3-fold Cu(1)), and 22/20.35 (4-fold Cu(1)). The presence of 3-fold Cu(1) sites suggests that the structural order of the present sample is not developed to so long rage, because such sites are allowed to appear only at terminals of a 4- or 2-fold coordinated chain.

3.3. Cu Knight Shift

Temperature dependences of the Knight shifts are plotted in Figs.5 and 6, for Cu(2) plane and Cu(1) chain sites, respectively. For both the sites, the c-axis can be taken as a principal axis of both the Knight shift tensors and the V_{zz} of EFG tensors.

For $x = 6.98$, the temperature dependences of the Knight shifts are very weak for both the principal directions, corresponding to the susceptibility. The values of Knight shifts are in good agreement for both Cu sites with the previous works (Kheinmaa *et al.*, 1988, Pennington *et al.*, 1989b, Takigawa *et al.*, 1989a and Barrett *et al.*, 1989).

For $x = 6.48$, the Knight shifts at Cu(2A) and Cu(2B) sites exhibit apparent temperature dependences for both the principal directions, corresponding to the

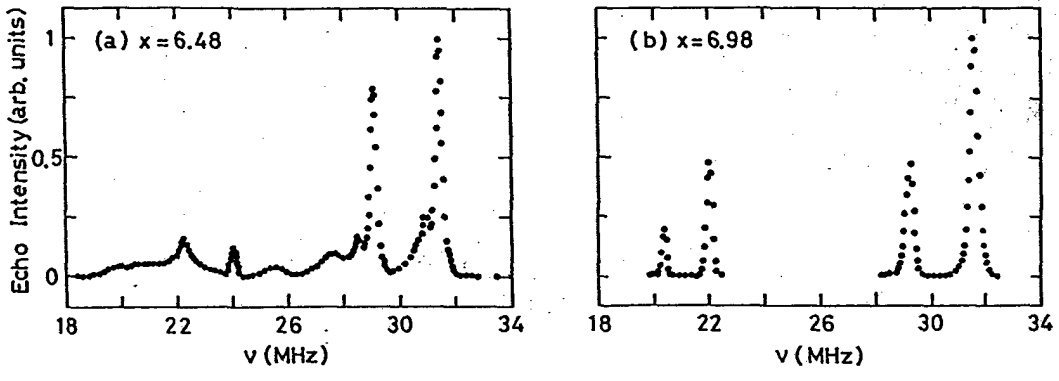

Fig.4. Cu NQR spectra taken in (a): $YBa_2Cu_3O_{6.48}$ and (b): $YBa_2Cu_3O_{6.98}$. The measurements have been done at 4.2 K in zero applied field.

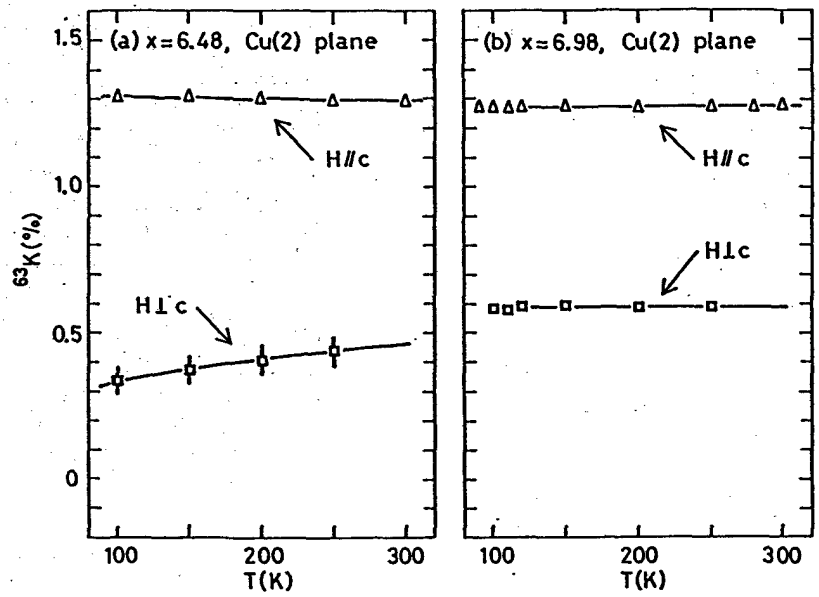

Fig.5. Temperature dependences of Cu Knight shifts at Cu(2) plane sites. (a): $YBa_2Cu_3O_{6.48}$. (b): $YBa_2Cu_3O_{6.98}$.

susceptibility. It should be noted here that, although the quadrupole frequencies are considerably different between the two sites Cu(2A) and Cu(2B) as shown in Fig.3(b), the Knight shifts are nearly the same. This result is similar to that found in $YBa_2Cu_3O_{6.75}$ by Horvatić *et al.*(1989a and 1989b). In our data, the difference in the NQR frequencies at the two sites is about 3 MHz and therefore about two times larger than the NQR line widths (1.4 MHz in FWHM), while possible difference in the Knight shift, if any, can be estimated to be at most 0.1 % *i.e.*, less than the NMR line width for H || c-axis (0.1 – 0.3 %). Possible difference in the temperature dependence of Knight shift has also been less than the distribution of each Knight shift value at all temperatures investigated here (100 K—300K). Thus, as far as the magnetic properties are concerned, we have no need to distinguish between the two Cu(2) plane sites.

Knight shift probes selectively unpaired electrons at the atom in concern. On the other hand, all electrons in the whole bands can be effective to EFG. The present experimental findings suggest that the structural difference in chain of the $x = 6.5$ phase gives rise to such a difference in the electronic structure as makes the EFGs at the two Cu(2) sites different, but does not so affect the magnetic electrons. This point will be refocused in the EFG analysis below section.

In the case of NMR at magnetic sites, the principal axes of the hyperfine coupling tensor and the susceptibility one are expected to coincide. Then we can write the relation between the Knight shft and the susceptibility, as follows,

$$K^{\alpha} = K^{\alpha}_{spin} + K^{\alpha}_{orb} \quad (\alpha = \parallel \; and \; \perp), \qquad (1a)$$

$$K^{\alpha}_{spin} = A^{\alpha}\frac{\chi^{\alpha}_{spin}}{N}, \qquad (1b)$$

$$K^{\alpha}_{orb} = 2\langle r^{-3}\rangle \mu_B \frac{\chi^{\alpha}_{orb}}{N}, \qquad (1c)$$

where N is the number of magnetic ions in a formula unit.

One should need the knowledge of single crystal data of susceptibility for a further analysis. However, any reliable measurements have not yet made of the single crystal susceptibilities for $YBa_2Cu_3O_x$ with varying oxygen concentration, because some paramagnetic second phase is involved as obtaining the single crystals. Instead, the anisotropic susceptibility measurements have been reported by taking advantage of high quality oriented powder samples for various oxygen concentrations (Nakazawa and Ishikawa, 1989 and Yamaguchi *et al.*, 1989). Since the temperature dependent part of the anisotropic susceptibility seems almost isotropic in their data, we can, in a good approximation, use our polycrystal data for χ to deduce the hyperfine coupling constant from the $K^{\alpha} - \chi$ plot diagram as shown in Figs.7 and 8. Then the slope of the $K^{\alpha} - \chi$ plot can be considered to correspond to the hyperfine coupling constant for the respective directions. In $YBa_2Cu_3O_x$ system, however, since the susceptibility arises from a contribution not only from Cu(2) plane sites but also from Cu(1) chains, we must estimate and separate the each Cu site contribution to the susceptibility.

In order to do this, we first note the fact that 2-fold and 3-fold Cu(1) chain sites are magnetically non-active Cu^{1+} ($3d^{10}$ configuration) ions. This fact has been found from the measurements of the nuclear spin lattice relaxation time T_1 and the Knight shft (Fig.6). The T_1 for those sites are extremely long (about three orders of magnitude) compared to the other sites, and the Knight shifts are relatively small and exhibit only a very weak temperature dependence. Therefore magnetically active copper ions can be taken to be limited to Cu(2) plane and 4-fold Cu(1) chain sites. Inspecting the NQR spectra shown in Fig.4(a), we can estimate that the abundance of 3-fold Cu(1) chain sites is roughly a tenth of that of 2-fold Cu(1), and therefore that the respective abundance of 2-, 3- and 4-fold Cu(1) chain sites is roughly 0.52 : 0.05 : 0.43 mole per formula unit of $YBa_2Cu_3O_{6.48}$. (In view of this fact, we can draw an interesting aspect about a relation between

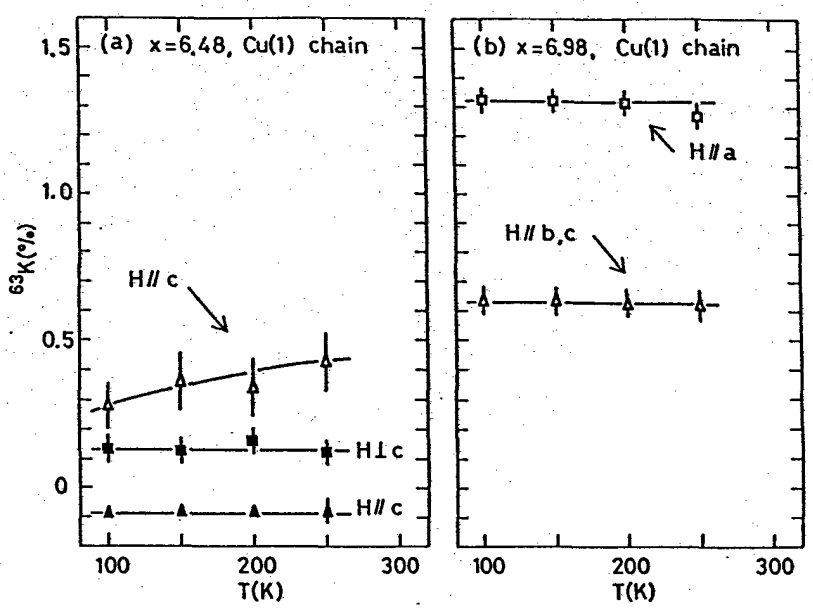

Fig.6. Temperature dependences of Cu Knight shifts. (a): Knight shifts at 4-fold (open triangle) and 2-fold (closed symbols) Cu(1) chain sites in $YBa_2Cu_3O_{6.48}$. (b): Knight shifts at 4-fold Cu(1) chain sites in $YBa_2Cu_3O_{6.98}$.

the hole (carriers) concentration p doped in the system and the oxygen content x. If we exclude the existence of 3-fold Cu(1) chain sites, abundance of 2- and 4-fold Cu(1) chain sites is given by $7-x$ and $x-6$, respectively, for $YBa_2Cu_3O_x$. Since the valence of each Cu site is then as; $Cu(2A)^{2+}$, $Cu(2B)^{2+}$, 4-fold $Cu(1)^{2+}$ and 2-fold $Cu(1)^{1+}$, we get $p=x-6$. On the opposite limit such as 3-fold Cu(1) chain sites are permitted as many as possible, we get $p=12-2x$ for $6.0<x<6.5$ and $p=1$ for $6.5<x<7.0$.)

Next, in order to separate the contributions from Cu(2) plane and 4-fold Cu(1) chain sites, we employ an estimation made by Mila and Rice (1989), in which the spin part contribution in the susceptibility is taken nearly equal between the two Cu^{2+} ion sites. This assumption can be verified in part by the $K-\chi$ plot shown in Fig.8.

Consequently, setting $N=2+0.43=2.43$ in eqs.(1), we obtain the hf coupling constants at Cu(2) sites from the $K^{\alpha}-\chi$ plot shown in Fig.7(a) and (b), as listed below,

$$A^{\parallel}=-21.3\pm 2 \quad \mathrm{kOe}/\mu_B\,, \qquad (2a)$$

$$A^{\perp}=168.2\pm 10 \quad \mathrm{kOe}/\mu_B\,. \qquad (2b)$$

These values are found nearly equal to those evaluated for $YBa_2Cu_3O_7$ (Takigawa *et al.*, 1989b and Barrett *et al.*, 1989). Thus, we find an interesting fact that, although the hole concentration differs by a factor of about two between the two phases $x=6.48$ and 6.98, the local electronic structure at Cu(2) plane sites is unaffected, to the extent of the present approximation, by introducing the holes. We note that a similar behavior has been found in ^{89}Y NMR which has been expected to probe selectively the electronic state within the planes (Alloul *et al.*, 1989).

In this connection, an investigation of the paramagnetic hf of the $x=6.0$ phase will be also of particular interest. Unfortunately, however, such an NMR observation may not be easy, because the Néel temperature (above 400 K) is rather high. Instead, the zero-field NMR spectrum has been observed in the antiferromagnetic state at T=4.2 K (Yasuoka *et al.*, 1988 and Mendels and Alloul, 1988). The Cu(2) electronic spins are ordered antiferromagnetically with the spin direction lying within the basal c-plane. The internal hf H_n has been obtained to be $\pm(79.65\pm 0.05)$ kOe. In order to obtain the hf coupling constant, we must take account of a possible spin reduction owing to the quantum fluctuations and/or the covalency effects of the magnetic electrons. Fortunately, the magnitude of ordered moment has been reported from neutron diffraction measurements to be $\langle S\rangle=(0.66\pm 0.07)\mu_B$ at 4.2 K (Tranquada *et al.*, 1988). Using this value, the hf coupling constant is given as follows,

$$A^{\perp}_{AF}=\frac{H_n}{\langle S\rangle}=\pm(120.7\mp 14) \quad \mathrm{kOe}/\mu_B\,, \qquad (2c)$$

where the subscript AF is to specify being the coupling constant in the case of the antiferromagnetic state. Hence, together with eq.(2b), we find a difference in the coupling constant as $A^{\perp}>A^{\perp}_{AF}$. The sign of $A^{\perp}_{AF}$, however, can not be determined from the present analysis alone. We give a further analysis to elucidate the mechanism of the hf in $YBa_2Cu_3O_x$ system below section, and therein show that the sign of $A^{\perp}_{AF}$ is most likely negative, *i.e.*, opposite to that in the paramagnetic state.

§4. Experimental Results for CuO

We have studied electronic states in CuO as a typical example of insulating antiferromagnet with Cu^{2+} ions. The Néel temperature has been reported to be 230 K from the neutron diffraction experiments (Forsyth *et al.*, 1988, Yang *et al.*, 1988) and the specific heat measurement (Junod *et al.*, 1989). The temperature dependence of susceptibility (Parkin *et al.*, 1988) looks very similar to that for $YBa_2Cu_3O_{6.0}$ (Johnston *et al.*, 1988).

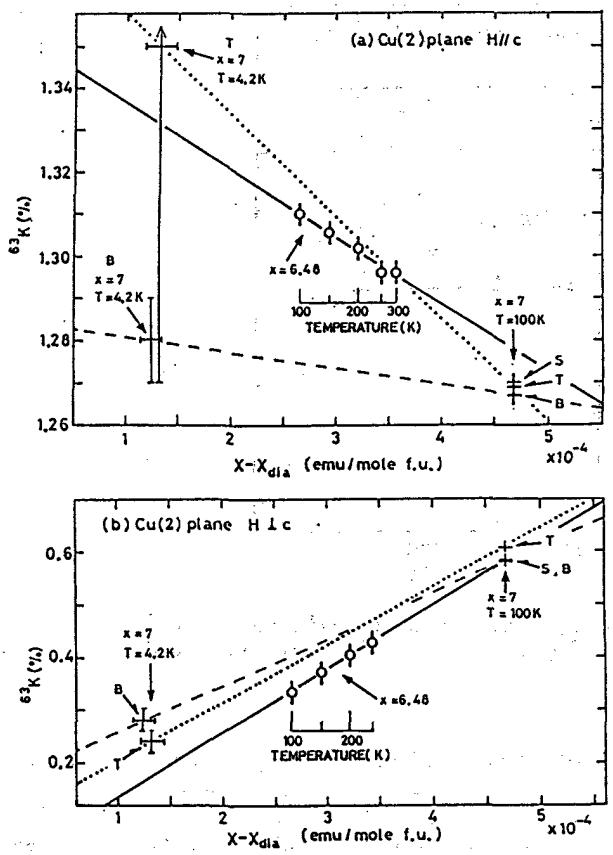

Fig.7. Cu Knight shifts at Cu(2) plane sites versus susceptibility, with temperature the implicit parameter. (a): H ∥ c-axis. (b): H ⊥ c-axis. The open circles are referred to the present data of $YBa_2Cu_3O_{6.48}$. The solid lines show the best fit thorough those data. The others indicated by $x = 7$ are referred to $YBa_2Cu_3O_{6.98}$ or the $T_c = 90$ K phase samples; The symbol S denotes the present datum taken at $T = 100$ K. The symbols of T show Takigawa *et al.*'s data (1989b) and the B Barrett *et al.*'s data (1989), taken at $T = 100$ and 4.2 K. The susceptibility is shown as the paramagnetic part subtracted by the diamagnetic contributions of core electrons.

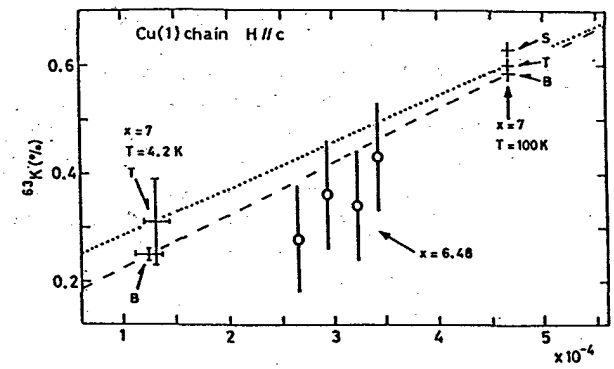

Fig.8. Cu Knight shifts at Cu(1) chain sites versus susceptibility, with temperature the implicit parameter. Only the Knight shft for H ∥ c-axis are shown. The open circles are referred to the present data of $YBa_2Cu_3O_{6.48}$. The others indicated by $x = 7$ are referred to the data of the $T_c = 90$ K phase samples ($YBa_2Cu_3O_{6.98}$); The symbol S denotes the present datum taken at $T = 100$ K. The symbols of T and B designate, respectively, Takigawa *et al.*'s data (1989b) and Barrett *et al.*'s data (1989), taken at $T = 100$ and 4.2 K. The susceptibility is shown as the paramagnetic part subtracted by the diamagnetic contributions of core electrons.

Not only the observation of Cu NMR in the antiferromagnetic state at 4.2 K (Tsuda *et al.*, 1988), but also we have successfully observed for the first time the Cu NMR signal in the paramagnetic state of CuO. Temperature dependence of the paramagnetic shift is shown in Fig.9. For CuO, we assume, for simplicity, the principal axes of the shift tensor and the EFG tensor are coincide. Although a monoclinic distortion is found in CuO (Åsbrink and Norrby, 1970), this assumption is appropriate as a first approximation for our purpose. It has been known that the principal z-direction of EFG is nearly normal to the square coordination of nearest neighbor four oxygens. We assume further the tetragonal symmetry for the shift tensor, and define $K^{\parallel} = K_{zz}$ and $K^{\perp} = K_{xx}$. Although single crystal data is, of course, necessary for the strict analysis, the essential feature extracted in the present study may not be altered.

Assuming that the temperature dependent part of susceptibility is isotropic, the polycrystal data of susceptibility can be used to deduce the hf coupling constant. From the $K^{\alpha} - \chi$ plot shown in Fig.10 with N=1, we get the following results,

$$A^{\parallel} = -146 \pm 10 \quad \text{kOe}/\mu_B\,, \qquad (3a)$$

$$A^{\perp} = \quad 15 \pm 15 \quad \text{kOe}/\mu_B\,. \qquad (3b)$$

Sine the antiferromagnetically ordered spin moments have been known to align nearly parallel to the direction of V_{zz} at each Cu site (Tsuda *et al.*, 1988), the above value of $A^{\parallel}$ in the paramagnetic state should be compared with the internal hf $H_n = \pm 121.5$ kOe/μ_B observed in the antiferromagnetic state. Using the neutron result of the ordered moment which has been reported to be $\langle S \rangle = (0.68 \pm 0.1)\mu_B$, the hf coupling constant in the antiferromagnetic state can be given as,

$$A^{\parallel}_{AF} = \frac{H_n}{\langle S \rangle} = \pm(178.7 \mp 23) \quad \text{kOe}/\mu_B\,. \qquad (3c)$$

We analyze in detail the mechanism of hf in CuO in the next section, and show the sign of $A^{\parallel}_{AF}$ to be negative and then being $A^{\parallel}_{AF} \leq A^{\parallel}$.

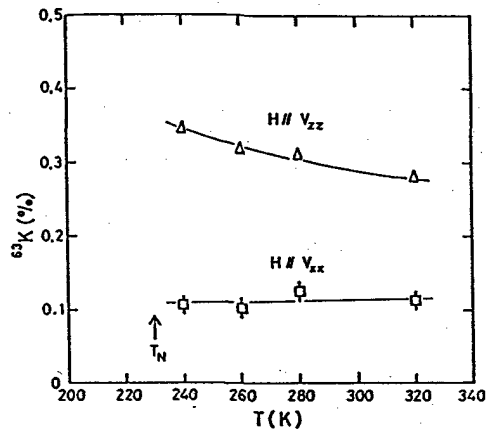

Fig.9. Temperature dependences of the paramagnetic (Knight) shifts of Cu NMR in CuO.

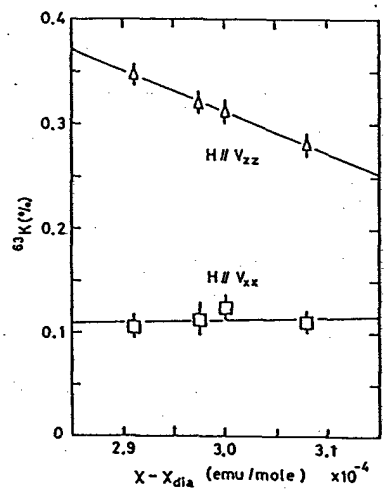

Fig.10. Cu paramagnetic (Knight) shift versus susceptibility for CuO, with temperature the implicit parameter.

§5. Hyperfine Field Analysis

5.1. General Expression of Hyperfine Field

From an analysis of the hf, we can obtain valuable information about the electronic state around the copper nuclei. As a useful starting point, we take a well-known ionic model appropriate to a Cu^{2+} ion in a tetragonal crystal field. The coupling constant of hf can be expressed in the model as follows (Abragam and Bleany, 1970),

$$A^{\parallel} = \langle r^{-3}\rangle\left\{-\kappa - \frac{4}{7} - \left(\frac{6\lambda}{7\Delta_1} + \frac{8\lambda}{\Delta_0}\right)\right\}, \quad (4a)$$

$$A^{\perp} = \langle r^{-3}\rangle\left(-\kappa + \frac{2}{7} - \frac{11\lambda}{7\Delta_1}\right), \quad (4b)$$

where in the first terms κ is a dimensionless parameter of the Fermi contact hf, the second terms, $-4/7$ and $2/7$ in eqs.(4a) and (4b), respectively, represent the dipole hfs produced by the ground state $|x^2-y^2\rangle$, and the last terms arise from the second order effect of the spin-orbit interaction, where λ is a spin-orbit coupling constant, Δ_0 is an energy separation between the ground state $|x^2-y^2\rangle$ and the first excited state $|xy\rangle$, and Δ_1 is that between $|x^2-y^2\rangle$ and the second excited states $|xz\rangle$ and $|yz\rangle$. Since the number of quantities to be resolved is more than the experimental knowns ($A^{\parallel}$ and $A^{\perp}$) in the present case, we have to make the following assumptions;

(I) The ratio of the two energy separations Δ_1 and Δ_0 ; $k \equiv \Delta_1/\Delta_0$ can be expected plausibly to lie in a rage of $k = 1.35 \pm 0.25$ (Abragam and Bleaney, 1970). We take the value of k as a parameter varying in this range.

(II) There appear, in a general expression of hyperfine interaction, two kinds of effective values of $\langle r^{-3}\rangle$, *i.e.*, the one is $\langle r_q^{-3}\rangle$ in an electric quadrupole interaction and the other is $\langle r_S^{-3}\rangle \equiv \langle r^{-3}\rangle$ in a magnetic hyperfine interaction. The two values can be deferred by a shielding effect of core electrons in the quadrupole interaction, as can be related with each other by,

$$\langle r_q^{-3}\rangle = (1-R)\langle r^{-3}\rangle, \quad (5)$$

where R denotes the shielding factor. It is difficult to evaluate the shielding effect for a specific material. Nevertheless, the shielding factor R is generally considered to be a small number and not so much sensitive to environment. We employ, in the present analysis, a Hartree-Fock value of R=0.1 reported by Freeman and Watson (1965).

By the use of assumption (I), each hf component to be resolved can be expressed as follows,

$$A_{Fermi} \equiv -\langle r^{-3}\rangle\kappa = -\frac{11}{56k-5}A^{\parallel} + \frac{56k+6}{56k-5}A^{\perp} - \frac{112k+56}{7(56k-5)}, \quad (6a)$$

$$A_{dip}^{\parallel} \equiv -\frac{4}{7}\langle r^{-3}\rangle, \quad (6b)$$

$$A_{dip}^{\perp} \equiv \frac{2}{7}\langle r^{-3}\rangle, \quad (6c)$$

$$A_{so}^{\parallel} \equiv -\left(\frac{6\lambda}{7\Delta_1} + \frac{8\lambda}{\Delta_0}\right)\langle r^{-3}\rangle = \frac{56k+6}{56k-5}(A^{\parallel} - A^{\perp} + \frac{6}{7}\langle r^{-3}\rangle), \quad (6d)$$

$$A_{so}^{\perp} \equiv -\frac{11\lambda}{7\Delta_1}\langle r^{-3}\rangle = \frac{11}{56k-5}(A^{\parallel} - A^{\perp} + \frac{6}{7}\langle r^{-3}\rangle). \quad (6e)$$

Only if the value of $\langle r^{-3}\rangle$ is known, every component can be evaluated as a function of the parameter k. We have obtained experimentally the value of $\langle r^{-3}\rangle$ by using assumption (II), as will be shown below.

5.2. Deduction of $\langle r^{-3}\rangle$

We have measured Cu quadrupole frequency ν_Q at Cu^{2+} ions in a variety of insulating copper oxides. Fig.11 (a) exhibits a plot of the observed ^{63}Cu quadrupole frequency ν_Q versus the calculated value of the EFG produced by the surrounding lattice ions. The evaluation of the lattice contribution to EFG has been made in a simple point charge model, taking account of all lattice points within a sphere of radius 50 Å at which a sufficient convergence is achieved (with a deviation of much less than 1%). We can find clearly from Fig.11(a) that the plots thus obtained lie along a straight line, over a wide range of substances. It should be noted here that, anticipating the nearly tetragonal symmetry of copper sites of our prime interest, this diagram is limited to the cases of nearly symmetric EFG with $\eta \leq 0.2$.

Let us consider physical meaning of this diagram. It is a key point to find out that a change in the degree of symmetry of the near neighbor coordination gives rise to a variation in the EFG, as can be seen in Fig.11(a). That is, (i) three oxides indicated by open circles exhibit the largest values of the lattice EFG and their Cu sites are of the 4-fold square coordinations, (ii) the intermediate group indicated by closed circles has the 5-fold pyramidal coordinations, (iii) the smallest EFG has been obtained for the 6-fold octahedral coordinations. Therefore we can easily find that the lattice contribution to EFG becomes smaller as the symmetry of coordination becomes like a cubic, as would be expected.

The present diagram suggests also that the value

of observed ν_Q results from a sum of two contributions from the d-shell of Cu^{2+} ion itself (ν_d) and the surrounding lattice ions (ν_{latt}), in agreement with the picture pointed out by Adrian (1988). This picture can be expressed as follows (Abragam and Bleaney, 1970),

$$\nu_Q = \nu_d + \nu_{latt}, \tag{7a}$$

$$\nu_d = \frac{3e^2Q}{2I(2I-1)h}\langle r_q^{-3}\rangle \langle L||\alpha||L\rangle l_{zz}, \tag{7b}$$

$$\nu_{latt} = (1-\gamma_\infty)\frac{3e^2QV_{zz}}{2I(2I-1)h}, \tag{7c}$$

where $\langle L||\alpha||L\rangle$ is the reduced matrix element of multiplit ^2D of Cu^{2+} ionic state, and evaluated by an algebraic calculation to be,

$$\langle L||\alpha||L\rangle = \frac{2}{21}, \tag{7d}$$

and l_{zz} represents the matrix element related to electronic quadrupole moment evaluated in the ground state $|0\rangle = |x^2-y^2\rangle$ as follows,

$$l_{zz} \equiv \langle 0|L_zL_z|0\rangle - \frac{1}{3}L(L+1) = 2, \tag{7e}$$

and V_{zz} in eq.(7c) denotes the maximum component of the lattice EFG tensor.

If we assume here that the values of $\langle r^{-3}\rangle$ and antishielding factor $1-\gamma_\infty$ is unchanged among these various oxides, then the present plots should obey a universal straight line, as is drawn in Fig.11(a). Then the intersection of the straight line with the vertical axis tells us readily the value of $\langle r^{-3}\rangle$ by using eqs.(5) and (7b), to be 6.28 ± 0.16 in atomic units (a.u.). This value corresponds to a reduction to 76.1% compared with that obtained by a Hartree-Fock calculation for a free Cu^{2+} ion (8.25 a.u., Freeman and Watson, 1965), being reasonable as would be expected for an ion in solids. The value of antishielding factor $1-\gamma_\infty$ is also given from the slope of the straight line by using eq.(7c), to be 21.6 ± 0.4. We tabulate the present results in table I.

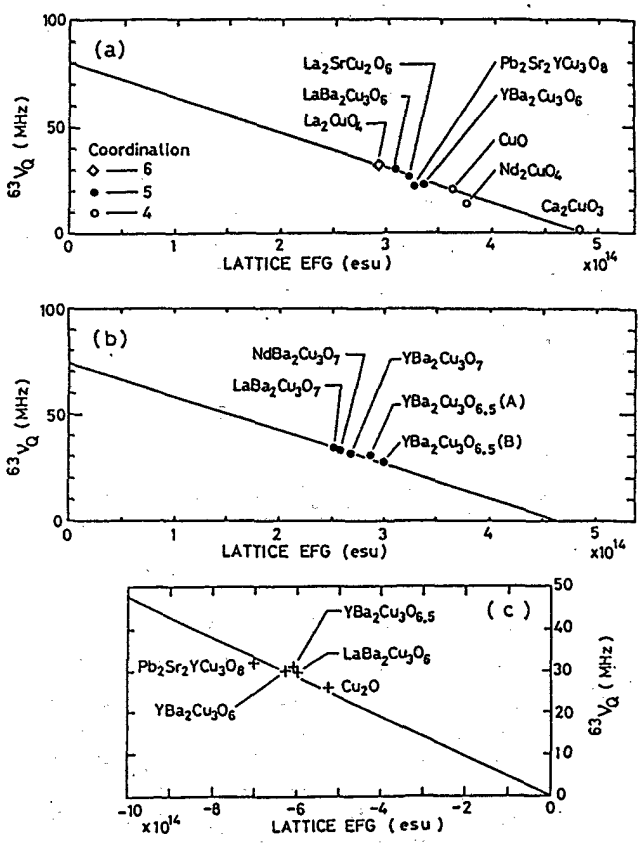

Fig.11. ^{63}Cu quadrupole frequency ν_Q is plotted as a function of the calculated value of the lattice contribution to the EFG at the copper sites. (a): 4-, 5- and 6-fold Cu^{2+} ions at planar sites in insulators. (b): 5-fold Cu^{2+} ions at planar sites in superconductors. (c): 2-fold Cu^{1+} ions in insulators. References of these data: La_2CuO_4 and CuO: Tsuda *et al.*(1988). $LaBa_2Cu_3O_6$, $Pb_2Sr_2YCu_3O_8$ and $LaBa_2Cu_3O_7$: Yoshimura *et al.*(1989). $La_2SrCu_2O_6$ and Ca_2CuO_3: the present work. $YBa_2Cu_3O_6$: Yasuoka *et al.*(1988) and Mendels and Alloul (1988). Nd_2CuO_4: Yoshinari *et al.*(1989). $YBa_2Cu_3O_7$ and $YBa_2Cu_3O_{6.5}$: Yasuoka *et al.*(1989). $NdBa_2Cu_3O_7$: Itoh *et al.*(1989).

Table I

Copper EFG parameters obtained by fitting the data in Figs.11. The definitions are given in eq.(6) in the text. The quadrupole frequencies ν_d are referred to ^{63}Cu nuclei and in the units of MHz. The expectation vales of $\langle r^{-3}\rangle$ are in the atomic units. The value of shielding factor $R = 0.1$ is assumed in the deduction of $\langle r^{-3}\rangle$ (see eq.(5)).

	Cu^{2+} Insulator	Cu^{2+} Superconductor	Cu^{1+}
ν_d	80.0 ± 2	74.0 ± 1	0
$\langle r^{-3}\rangle$	6.28 ± 0.16	5.81 ± 0.08	
$1-\gamma_\infty$	21.6 ± 0.4	20.5 ± 0.2	6.3 ± 0.1

5.3. Hyperfine Field Analysis for CuO

We have used this value of $\langle r^{-3}\rangle$ to evaluate the hf coupling constants in CuO. Although depending on the parameter k defined in assumption (I), a unique result has been obtained from eqs.(6), as shown in table II. Every contribution is very reasonable in both sign and magnitude, comparable to the literature data of Cu^{2+} ion EPR and NMR in various well-studied insulators. For a typical example, the reported EPR results of Cu^{2+}:MgO are also shown in table II. It is meaningful for us to keep in mind that the negative value of A_{Fermi} arises from the core polarization mechanism as would be usually expected in transition metal compounds. We can conclude from the present results that the electronic state of Cu^{2+} ions in CuO can be understood in terms of a usual model appropriate to a simple insulator.

In Figs.12(a) and (d), we depict schematically the constitution of the hf coupling constants obtained by the present analysis. Since the ionic picture provides a good approximation for CuO, it is natural to expect that these coupling constants are basically unchanged between the paramagnetic and the antiferromagnetic states. Then

Table II

The coupling constants and parameters of copper hyperfine field in CuO and at Cu(2) plane sites in $YBa_2Cu_3O_{6.48}$. The definitions are given in eqs.(1), (4) and (6) in the text. The hyperfine coupling constants are in the units of kOe/μ_B. Also shown are the values of EPR results of Cu^{2+}:MgO (Coffman, R., 1968) and of the results obtained for $YBa_2Cu_3O_7$ (Takigawa *et al.*, 1988b and Mila and Rice, 1989). In the analysis made by Mila and Rice, the values of $\langle r^{-3}\rangle$ and κ are assumed.

	Cu^{2+}:MgO	CuO	$YBa_2Cu_3O_{6.48}$	$YBa_2Cu_3O_7$
$A^{\parallel}$		-146 ± 10	-21.6 ± 1	-41.2
$A^{\perp}$		15 ± 15	168.2 ± 10	191.1
$\langle r^{-3}\rangle$	5.46	6.28 ± 0.16	5.81 ± 0.10	6.30
A_{Fermi}	-90.8	-125 ± 15	62.2 ± 10	58.1
κ	0.266	0.318 ± 0.04	-0.125 ± 0.02	0.325
$A^{\parallel}_{dip}$	-195.1	-225 ± 6	-208 ± 4	-229.9
$A^{\perp}_{dip}$	97.5	112 ± 3	104 ± 2	114.9
$A^{\parallel}_{so}$	145.1	203 ± 20	157 ± 15	130.6
$A^{\perp}_{so}$	25.75	27.4 ± 5.0	21 ± 5.0	18.1
$\frac{\lambda}{\Delta_0}$	-0.066	-0.060 ± 0.002	-0.045 ± 0.001	-0.038

we can plausibly determine the sign of $A^{\parallel}_{AF}$ in eq.(3c) to be negative.

5.4. Hyperfine Field Analysis for Cu(2) Plane Sites in $YBa_2Cu_3O_{6.48}$

The value of $\langle r^{-3}\rangle$ can be obtained in the same way as the above mentioned insulating case. There arises in the metallic case, however, an essential difficulty in evaluating the valence of each ion. Fortunately in the present material, we can expect, from a chemical consideration, the ionic characters of Y^{3+} and Ba^{2+} to be relatively firm. Thus the difficulty can be reduced to a problem how to settle a charge distribution within the sublattice of copper and oxygen ions. Photoemission studies have revealed that the extra holes in the superconducting phases are accommodated mainly at oxygen sites and also that the copper ions are stable in Cu^{2+} charged state but not in Cu^{3+} (Fujimori *et al.*, 1987a and 1987b, Bianconi *et al.*, 1987 and Nücker *et al.*, 1988). In addition, recent ^{17}O-NMR data in $YBa_2Cu_3O_7$ (Takigawa *et al.*, 1989c) are consistent with the assumption that the extra holes are distributed at every oxygen site in roughly equal population.

Consequently we adopt, as a crude estimation, a point charge model in which the valences are assumed as follows; Y^{3+}, Ba^{2+}, $Cu(1)^{2+}$, $Cu(2)^{2+}$ and $O^{-13/7}$ for all oxygens, so as to calculate the EFG at Cu(2) sites. The calculations have been performed for three oxide superconductors $RBa_2Cu_3O_{7.0}$ (R=Y, La and Nd). Together with the calculated value of EFG obtained in this way, the observed quadrupole frequency gives a plot shown in Fig.11 (b). In the same way as the preceding analysis for the insulating case, fitting to a straight line through the three points, we get, $\langle r^{-3}\rangle = 5.81 \pm 0.08$ (a.u.) and $1-\gamma_\infty = 20.5 \pm 0.2$, as shown in tableI. These values of $\langle r^{-3}\rangle$ and $1-\gamma_\infty$ exhibit just slight reductions by less than 10% compared with the insulating case. In view of the apparent change in the bulk properties from an insulating phase to a superconducting one, these similarities found here are somewhat surprising. From this fact, we are intended to argue that the local electronic structure at Cu(2) plane sites in the superconducting phase is rather close to that in the insulating phase.

By using this value of $\langle r^{-3}\rangle = 5.81$ (a.u.), we have evaluated the details of the hf in $YBa_2Cu_3O_{6.48}$. The results are shown in table II, and illustrated schematically in Figs.13(a) and (c). We can see, from the present results, that, although the values of $\langle r^{-3}\rangle$ (therefore A^{α}_{dip}) and spin-orbit (A^{α}_{so}) contributions are similar to the usual case of Cu^{2+} ions, the Fermi contact contribution (A_{Fermi}) is quite strange in both sign and magnitude. Considering the two similarities found between the superconducting phase and the insulating one in the EFG parameters ($\langle r^{-3}\rangle$ and $1-\gamma_\infty$) and in the anisotropic parts of the hf (dipole and spin-orbit contributions), we can rather expect that a similar contribution from the usual core polarization mechanism should be hidden in the A_{Fermi} of $YBa_2Cu_3O_{6.48}$ as well. Then the present result indicates that there is a certain additional contribution to the Fermi contact part of hf in $YBa_2Cu_3O_{6.48}$, which is a large and positive one and has never been found before among the transition metal compounds (involving metals and insulators).

This anomalous contribution also seems quite similar to the results obtained for the $x = 7$ phase of $YBa_2Cu_3O_x$ by Takigawa *et al.*(1989b) and Mila and Rice, (1989). It is also obvious from the above subsection that such an anomalous hf does not appear in CuO. Thus, our particular interest is turned to a problem to elucidate the origin of this anomalous hf characteristic of $YBa_2Cu_3O_x$ system.

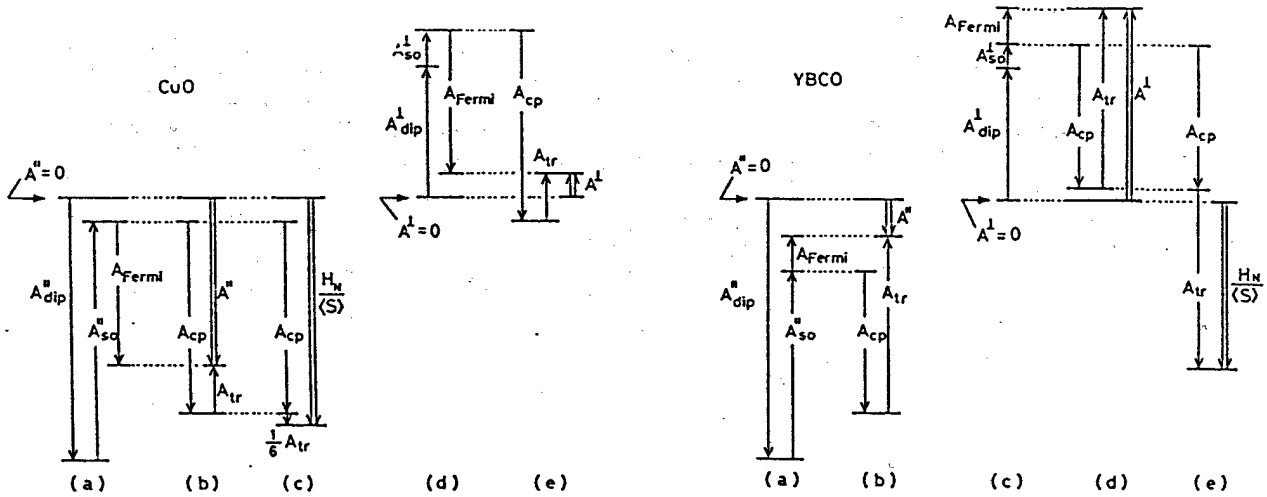

Fig.12. Diagrams showing the constitution of the hyperfine field couplings in CuO. The decomposition shown in (a) and (d) is based on the results in table II. The further decomposition of the component A_{Fermi} into A_{cp} and A_{tr} is shown in (b) and (e) for the paramagnetic state and (c) for the antiferromagnetic state. The composition into A_{cp} and A_{tr} are based on the diagram shown in Fig.15 and on the discussion given in the text. The double arrows shown in (b), (c) and (e) denote the hyperfine field couplings which have been observed experimentally.

Fig.13. Diagrams showing the constitution of the hyperfine field couplings in $YBa_2Cu_3O_x$ system. It is shown in the text that all these couplings are nearly unchanged between $6.0 \leq x \leq 7.0$. The decomposition shown in (a) and (d) is based on the results in table II. The further decomposition of the component A_{Fermi} into A_{cp} and A_{tr} is shown in (b) and (d) for the paramagnetic (normal) state of $x = 6.48$ and (e) for the antiferromagnetic state of $x = 6.0$. The composition into A_{cp} and A_{tr} are based on the diagram shown in Fig.15 and on the discussion given in the text. The double arrows shown in (b), (d) and (e) denote the hyperfine field couplings which have been observed experimentally.

§6. Origin of the Anomalous Hyperfine Field

6.1. General Consideration

A no-interacting ionic model is obviously inadequate to account for the anomalous hf. In addition, the origin can not be ascribed to the doped holes (carriers), because a similar anomalous hf is, as will be shown below, present in the insulating phase $x = 6.0$ as well. Thus we are impelled to look for the origin in the effects of covalent bonding and/or overlap between the relevant orbitals. There are, in principle, three candidates responsible for the positive Fermi contact hf. All of them involves an electron transfer process via the covalency between a ligand orbital and a copper orbital, and therefore being a kind of transferred hf.

(A) The ligand oxygen ion can be polarized in spin by a covalent electron transfer from the ligand into the unoccupied 3d-orbital of adjacent Cu^{2+} ion (say, the left copper site shown in Fig.14(A)). This polarized ligand spin is transmitted into a nominally empty 4s orbital at the other side of Cu^{2+} ion via the covalency between the ligand orbital and the Cu 4s orbital. In this process, the 4s spin induced at the right copper site is inevitably parallel to the 3d spin of the left copper ion, as far as the transfer Hamiltonian is spin independent. Hence this contribution to the hf should change its own sign depending on whether the spin alignment of neighboring Cu^{2+} ions is parallel or antiparallel. The hyperfine interaction due to process A is what is called the "supertransferred hyperfine interaction" (originally studied by Kamimura, 1966, Huang *et al.*, 1967, and Taylor *et al.*, 1973 and reviewed by Šimánek and Šroubek, 1972).

(B) The ligand electron can be virtually transferred into nominally empty 4s orbitals of a Cu^{2+} ion via the covalency between them. There are two possible channels for this transfer process, corresponding to the 4s orbitals with different spin directions as illustrated in Figs.14(B1) and (B2). The 3d-4s exchange interaction makes a difference in the transfer probabilities for the two channels, leading to a preference of process B1 over B2 in Fig.14. This preferential transfer gives rise to a net spin density at the copper nuclear site oriented parallel to the 3d spin, and leaving behind a net spin at the ligand orbital oppositely directed from the 3d spin. This mechanism is what is called the "exchange polarization of bonding orbital" (Watson and Freeman, 1961, Šimánek and Müller, 1970 and Šimánek and Šroubek, 1972).

(C) The ligand is polarized by the same process as mentioned in the first step of process A. The core electrons (1s, 2s and 3s) at the right Cu^{2+} ion can be polarized by the overlap effect between the polarized ligand and the core electrons. Like process A, we get also in this process the net spin polarized parallel to the 3d spin at the left Cu^{2+} ion. This process, however, can not be of prime importance, because this process is inadequate to explain the observed difference in A_{Fermi} between CuO and $YBa_2Cu_3O_x$ system. The overlap of the ligand orbitals with the cores of Cu^{2+} ion is expected to be greater for CuO than $YBa_2Cu_3O_x$ system, because of the relatively short bond lengths. This fact gives rise to a tendency contrary to the present experimental findings. Therefore we can rule out the possibility of process C.

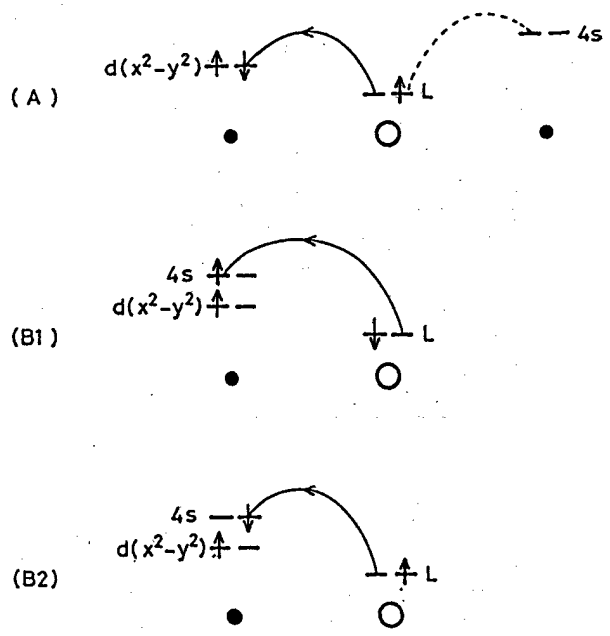

Fig.14. Schematic illustrations of process A (A) and process B (B1 and B2). The solid circles denote the copper ions and open circles the oxygen ions. The ligand orbitals L are primarily the hybrids of 2s and 2p orbitals. Two channels (B1 and B2) are present in process B.

In what follows, we consider only processes A and B. We can rewrite the coupling constant of the Fermi contact hf as follows,

$$A_{Fermi} = A_{cp} + \sum_i (\pm 1)^p a_{tr}(i), \qquad (8)$$

where A_{cp} denotes the contribution arising from usual core polarization mechanism and a_{tr} the anomalous contribution originating from the above mentioned electron transfer process of either A or B, i represents the nearest neighbor Cu^{2+} (O^{2-}) sites corresponding to process A(B), $-(+)$ sign is taken correspondingly to process A(B), and p is defined by the spin direction of neighboring Cu^{2+} ions as $p = 1$ if antiparallel and $p = 2$ if parallel. When applying an external field in the paramagnetic state, we get $p = 2$ irrespective of which process (A or B). It is therefore convenient to define the total amount of anomalous contributions observed in paramagnetic state, as follows,

$$A_{tr} \equiv \sum_i a_{tr}(i). \qquad (9)$$

We extract the values of A_{tr} in $YBa_2Cu_3O_x$ and CuO from our experimental data, as shown below.

6.2. Analysis for $YBa_2Cu_3O_x$

For the paramagnetic state ($x = 6.48$), inserting the values of A_{tr} shown in table II into eq.(8), we obtain the following relation,

$$A_{cp} + A_{tr} = 62.2 \pm 10 \quad \mathrm{kOe}/\mu_B. \qquad (10)$$

This equation defines the region P in the A_{cp} versus A_{tr} diagram shown in Fig.15(a).

For the antiferromagnetic state ($x = 6.0$), taking account of four nearest neighbor Cu^{2+} spins within the same plane, we can rewrite eq.(4b) by using eqs.(6) and (8) as follows,

$$A_{cp} \mp A_{tr} + A^{\perp}_{dip} + A^{\perp}_{so} = A^{\perp}_{AF}, \qquad (11)$$

where $-(+)$ sign of A_{tr} term corresponds to process A(B). The values of $A^{\perp}_{dip}$ and $A^{\perp}_{so}$ are unknown for $x = 6.0$. We assume here, in a good approximation, that A^{α}_{dip} and A^{α}_{so} are relatively insensitive to oxygen content x, because they have been found to retain the ionic values even in the superconducting phase as mentioned earlier. Then we have estimated the vales of $A^{\perp}_{dip}$ and $A^{\perp}_{so}$ merely by taking account of the difference in the value of $\langle r^{-3} \rangle$ between the superconducting phase and the insulating one. The negative (positive) value of $A^{\perp}_{AF}$ shown in eq.(2c) is taken to correspond to process A(B). Inserting those values into eq.(11), we get,

$$A_{cp} - A_{tr} = -256 \pm 20 \quad \mathrm{kOe}/\mu_B, \qquad (12a)$$
$$A_{cp} + A_{tr} = -15 \pm 20 \quad \mathrm{kOe}/\mu_B, \qquad (12b)$$

for processes A and B, respectively. Eqs.(12a) and (12b) define respectively the regions AFA and AFB in Fig.15(a).

If we set a specific value of A_{cp}, then A_{tr} is determined from Fig.15(a) as a segment of the corresponding horizontal line across the regions, P, AFA and AFB. Now we use the value $A_{cp} = -121 \pm 10$ (kOe/μ_B), reported for various compounds containing Cu^{2+} ions (Abragam and Bleaney, 1970). The allowed value for A_{tr} is then obtained from eqs.(10), (12a) and (12b) and can be illustrated as the hatched area in Fig.15(a). The results are summarized in table III. Since the transferred hf seen by the copper nuclei is produced by the 4s electrons for both processes A and B, we can also express the amount of this hf in terms of a fraction of the unpairing 4s spin. Using the reported value $H_{4s} = 2598$ (kOe) for neutral copper atom ($3d^{10}4s^1$) which has been obtained by the atomic beam magnetic resonance method (Ting and Lew, 1957), we obtain the values of 4s spin fraction f_{4s} as are also shown in table III.

We want to emphasize the fact that there should exist a similar anomalous A_{tr} even in the insulating phase $x = 6.0$. This fact clearly demonstrates that this anomalous hf does not arise from the extra holes (carriers) existing in the superconducting phase, but must be an inherent nature of $YBa_2Cu_3O_x$ ($6.0 \leq x \leq 7.0$) system.

6.3. Analysis for CuO

A similar analysis can be applied to CuO. For the paramagnetic state, we use the following relation instead of eq.(10),

$$A_{cp} + A_{tr} = -125 \pm 15 \quad \mathrm{kOe}/\mu_B. \qquad (13)$$

This equation defines the region P' as shown in Fig.15(b).

For the antiferromagnetic state, taking account of the spin structure (among the nearest neighbor twelve

Table III

The transferred hyperfine field coupling A_{tr} and the fraction of the unpairing 4s spin f_{4s}. A_{tr} are in the units of kOe/μ_B, and f_{4s} in %. The values shown here correspond to the hatched area in Fig.15. The value of $A_{Fermi} = -121 \pm 10$ kOe/μ_B is assumed in the present deduction of A_{tr}. Also shown are the results of $YBa_2Cu_3O_7$ (Mila and Rice, 1989), in which only process A is considered.

		CuO	$YBa_2Cu_3O_{6.0}$	$YBa_2Cu_3O_{6.48}$	$YBa_2Cu_3O_7$
Process A	A_{tr}	0 – 20	135 ± 30	183 ± 20	186
	f_{4s}	0 – 0.8	5.2	7.0	7.2
Process B	A_{tr}	0 – 10	106 ± 30	183 ± 20	
	f_{4s}	0 – 0.4	4.1	7.0	

Cu^{2+} spins, seven spins are coupled antiferromagnetically and five spins ferromagnetically, Forsyth *et al.*, 1988 and Yang *et al.*, 1988), we get,

$$A_{cp} - \frac{1}{6}A_{tr} = -162 \pm 42 \quad \text{kOe}/\mu_B, \qquad (14a)$$

$$A_{cp} + A_{tr} = -162 \pm 42 \quad \text{kOe}/\mu_B, \qquad (14b)$$

for processes A and B, respectively. Eqs.(14a) and (14b) define the regions AFA' and AFB', respectively, as shown in Fig.15(b).

Constraining the value of A_{cp} to be within a region of $A_{cp} = -121 \pm 10$ (kOe/μ_B) as done for above mentioned $YBa_2Cu_3O_x$, we obtain the allowed value for A_{tr} to be 0–20 (kOe/μ_B) as shown in table III and by a hatched area in Fig.15(b). This value is an expected one for usual transition metal compounds

6.4. Origin of the Anomalous Hyperfine Field

The most decisive method to resolve which process (A and B) governs the anomalous transferred hf may be to determine experimentally the sign of A_{AF} in eq.(2c). Unfortunately, however, we can not obtain any information about the sign from the present experimental data alone. Nevertheless, if we take notice of the ^{17}O-NMR data reported by several groups, process A is turned out to be most likely, as shown below. It can be readily found from Fig.14 that the sign of the hf at the oxygen site is different between two processes A and B. The ^{17}O-NMR data for $6.5 \leq x \leq 7$ have shown that the hf coupling constants are large and positive (Takigawa *et al.*, 1989c, Kitaoka *et al.*, 1989 and Oldfield *et al.*, 1989). The core polarization mechanism due to 2p spin is generally known to result in a positive Fermi contact hf. Hence, whether the character of the polarized ligand orbital is 2s or 2p, the signs of the hfs are the same. We thus arrive at a conclusion that process A prevails in $YBa_2Cu_3O_x$ system.

Consequently, the allowed value for A_{tr} in $YBa_2Cu_3O_x$ can be determined to lie in the regions P and AFA as follows,

$$A_{tr} = \begin{cases} 183 \pm 20 & (x = 6.48), \qquad (15a) \\ 135 \pm 30 & (x = 6.0). \qquad (15b) \end{cases}$$

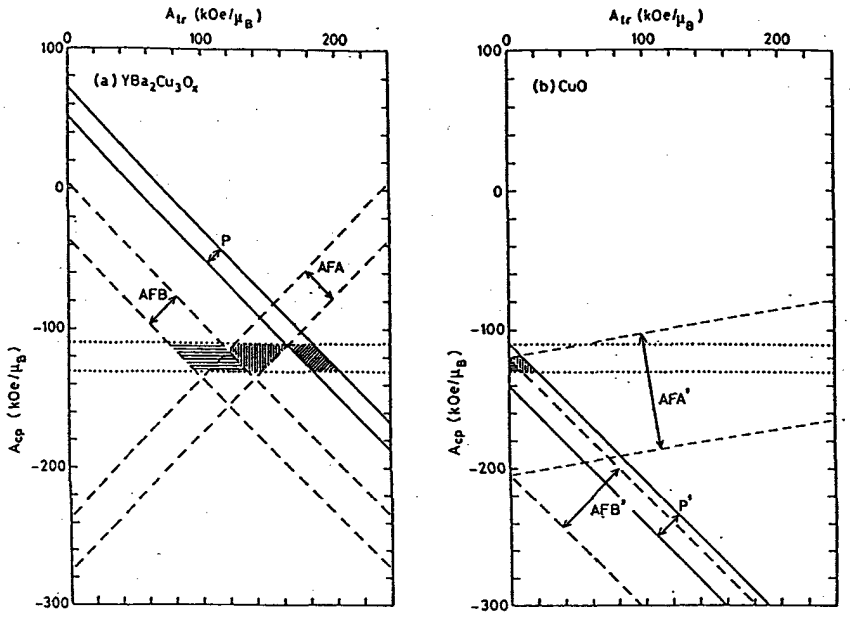

Fig.15. Diagram of A_{cp} versus A_{tr}, (a) for $YBa_2Cu_3O_x$ system and (b) for CuO. The region designated by a pair of doted lines is referred to the assumed value of $A_{cp} = -121 \pm 10$ (kOe/μ_B).

The individual contribution from a spin $\frac{1}{2}$ of a single nearest neighbor ion to the transferred hf is 34–46 (kOe/μ_B), being an order of magnitude larger compared with the literature data reported for various transition metal compounds (Watson and Freeman, 1961, Kamimura, 1966, Huang *et al.*, 1967, Locher *et al.*, 1970, Šimánek and Müller, 1970 and Taylor *et al.*, 1973). Within the experimental errors and the approximations involved in the present analysis, we can not determine whether or not the value of A_{tr} is actually dependent on the oxygen concentration x. In any case, we find surely an outstanding feature inherent in $YBa_2Cu_3O_x$ ($6.0 \leq x \leq 7.0$) system that the covalent electron transfer (process A) is extremely active compared with in the other usual compounds such as CuO.

Based on these results, we can complete the diagram showing the constitution of the hf components, as shown in Fig.12(b), (c) and (e) for CuO and Fig.13(b), (d) and (e) for $YBa_2Cu_3O_x$ system.

6.5. Difference between $YBa_2Cu_3O_x$ and CuO

The band theory predicts a d-band metal for both $YBa_2Cu_3O_{6.0}$ and CuO (Oguchi *et al.*, 1987 and Park *et al.*, 1988), in marked contrast to the actual states. This seems to suggest an importance of the electronic correlations in both the materials. There have also been found experimentally considerable similarities between $YBa_2Cu_3O_{6.0}$ and CuO in several electronic properties. There is, however, an essential difference between the two; $YBa_2Cu_3O_{6.0}$ becomes superconductor by the hole doping, whereas CuO has not shown superconductivity as any holes are introduced. In addition, the present study reveals a noticeable feature in $YBa_2Cu_3O_{6.0}$ of the charge fluctuations of process A. Therefore we can find that, even in the insulating phase $YBa_2Cu_3O_{6.0}$, the underling electronic state is already markedly different from a usual insulator such as CuO. Considering the fact that the local electronic states at the Cu^{2+} sites have been approximately invariant for $6.0 \leq x \leq 7.0$, we are intended to argue that, in the insulating phase, the underlying electronic state is ready for the superconductivity. Thus, it seems rather crucial to elucidate the mechanism which gives rise to the difference between the insulator $YBa_2Cu_3O_{6.0}$ and a usual insulator such as CuO. It will be shown below that this arises in part from the difference in the crystal structure of these materials.

Process A involves the covalent electron transfer from the ligand to the unoccupied 3d orbital of Cu^{2+} ion, as can be written by $\{3d^9\} \longrightarrow \{3d^{10}L\}$, where L denotes a ligand hole. According to the Heitler-London method in the molecular orbitals model, the degree of this transfer can be measured by the so-called covalency parameter γ given as follows (Abragam and Bleaney, 1970),

$$\gamma = \frac{\langle d^9 \,|\, d^{10}L \rangle \, \langle d^9 \,|\, H \,|\, d^9 \rangle - \langle d^9 \,|\, H \,|\, d^{10}L \rangle}{\langle d^{10}L \,|\, H \,|\, d^{10}L \rangle - \langle d^9 \,|\, H \,|\, d^9 \rangle}, \qquad (16a)$$

where H is the relevant Hamiltonian, and the energy denominator is nothing but what is called the charge transfer gap Δ (Fujimori and Minami, 1984, Hüfner, 1985 and Zaanen and Sawatzky, 1987),

$$\Delta = \langle d^{10}L \,|\, H \,|\, d^{10}L \rangle - \langle d^9 \,|\, H \,|\, d^9 \rangle \,. \qquad (16b)$$

The energy gap Δ is required to bring out the charge fluctuations of $\{3d^9\} \longleftrightarrow \{3d^{10}L\}$. While it is difficult to evaluate the numerator of eq.(16a), the denominator (*i.e.*, eq.(16b)) can be obtained from the valence band XPS experiments and theoretical calculations (such as a band calculation and a cluster configuration interaction method). The results reported by the XPS (Shen *et al.*, 1987) and the band calculation (Park *et al.*, 1988) are shown in table IV. The value of the charge transfer gap Δ is found to be systematically smaller for $YBa_2Cu_3O_x$ system than CuO, consistent with the present NMR results. The tendency observed experimentally in Δ seems to be related closely to the crystal structures, because the same tendency is also found from the band calculation.

Table IV

The charge transfer gaps Δ (in eV) obtained by the XPS experiments (Shen *et al.*, 1987) and the band theory (Park *et al.*, 1988).

	CuO	$YBa_2Cu_3O_6$	$YBa_2Cu_3O_7$
XPS	1.0		0.5
Theory	1.66	0.36	0.20

The ligand orbital relevant to process A can be expressed primarily by a linear combination of oxygen 2s and $2p_\sigma$ orbitals. Therefore process A should be sensitive to the Cu^{2+}—O^{2-}—Cu^{2+} bridging angle ϕ. It can be conjectured that a linear bond $\phi = 180°$ is more favorable to process A than a $\phi = 90°$ bond. Thus we can expect that this process is much active in the perovskite type structure (*i.e.*, a corner-sharing net-work in a [–CuO_2–] sheet), compared with in a type of edge-sharing net-work appearing in CuO. The charge fluctuations in process A is inevitably accompanied by spin fluctuations. Since it is well known that the character of magnetic interaction between Cu^{2+} ions is dependent essentially on the bridging angle ϕ (Hay *et al.*, 1975 and Willett and Landee, 1981), it can be expected that both the fluctuations in charge and spin take place in such a manner as reflecting the value of ϕ. Considering that all of the high T_c oxides has been of the layered perovskite type structure, the electronic state inherent in this structure seems to play a vital role in the superconductivity as well, as was originally pointed out by Pauling (1987).

§7. Empirical Rule of EFG in Copper Oxides

7.1. Relation between Observed ν_Q and Lattice EFG

As shown in Figs.11(a) and (b), a linear relation is found between the quadrupole frequencies observed at Cu^{2+} ions and the EFGs produced by the surrounding lattice ions. We have also found the similar relation for the sites of 2-fold Cu^{1+} ions in various oxides, as shown in Fig.11(c). The data can be fitted to a straight line through the origin, and yield the EFG parameters of eq.(6) as $\nu_d = 0$ MHz and $1 - \gamma_\infty = 6.3 \pm 0.1$. The null value of ν_d is, of course, to be expected for the case of non-magnetic Cu^{1+} ($3d^{10}$ configuration) ions. The value of antishielding factor $1 - \gamma_\infty = 6.3$ is smaller by a factor of 2.8 than a theoretical value 17.6 obtained by a Hartree-Fock calculation (Freeman and Watson, 1965). We summarize these results in table I, together with the results for Cu^{2+} ion as mentioned earlier.

Table I and eqs.(6) allow us to predict the copper quadrupole frequency to be observed at a given Cu site in any Cu oxide, only if the lattice parameters, the lattice point and the valence of each ion are known from diffraction experiments. The conditions on which the present relation holds are as follows; (i) the asymmetry is small as $\eta \leq 0.2$ is satisfied, (ii) excepting the non-stoichiomeric composition such as $La_{2-x}Sr_xCuO_4$ ($0 \leq x \leq 0.2$). The failure in the highly asymmetric sites reflects the fact that we assume the ground state to be purely of $|x^2 - y^2\rangle$ in the evaluation of eq.(6b) and (6e). The failure in $La_{2-x}Sr_xCuO_4$ suggests that the lattice parameters and the lattice points determined by a diffraction technique correspond to the averaged values taken over a coherence length of the particle used in the technique, but not to the local values seen by the resonance technique such as NQR.

7.2. The Application to Site Assignment

The high field NMR measurement has revealed the value of asymmetry parameter η to be about 0.9 for the two ^{63}Cu NQR lines at 24 MHz and 22 MHz and 0 for the three lines at 31.4MHz, 30.6 MHz and 27.8 MHz. The highly asymmetric value of η is characteristic of 4-fold and 3-fold coordinated Cu(1) chain sites (Lütgemeier, 1988 and Yasuoka *et al.*, 1989). Inspecting the concentration dependence (Yasuoka *et al.*, 1989) of the intensities of 24 and 22 MHz lines, they have been assigned to be 3-fold and 4-fold Cu(1) sites, respectively. On the other hand, the lines with $\eta = 0$ can be expected for Cu(2A) and Cu(2B) sites and 2-fold Cu(1) sites, because the symmetry of their sites are nearly tetragonal.

The calculation of lattice EFG in a point charge model yields the results of (V_{aa}, V_{bb}, V_{cc}) in the units of e.s.u., as follows;

$$\begin{aligned} \text{Cu(2A)} &: (-1.53, -1.34, 2.86), \\ \text{Cu(2B)} &: (-1.65, -1.34, 2.99), \\ \text{2-fold Cu(1)} &: (2.94, 3.10, -6.04). \end{aligned}$$

Using these values together with the diagram shown in Fig.11(b) and (c), we can resolve the problem of site assignment for Cu NQR lines in $x = 6.48$. 2-fold Cu^{1+} ions should appear along the straight line shown in Fig.11(c). This restriction allows exclusively the line of 31.4 MHz to be 2-fold Cu(1) sites. Next, we can draw in Fig.11(b) two vertical lines located at each calculated value of the lattice EFG corresponding to Cu(2A) and Cu(2B) plane sites. Two intersections are obtained of these two vertical lines with the universal line drawn in Fig.11(b). It can easily found that the quadrupole frequencies indicated by the intersections are very close to the observed NQR lines of 30.6 and 27.8 MHz in $x = 6.48$. Thus we obtain, in a clear manner, a unique result of the site assignment as follows; 30.6 and 27.8 MHz lines come from Cu(2A) and Cu(2B) sites, respectively.

7.3. The Application to NQR Line Width

Consideration of the antishielding effect provides an interesting aspect on the NQR line width shown in Fig.4 (a). Inhomogeneous line width of an NQR spectrum arises mainly from lattice imperfection. The possible lattice imperfection in $YBa_2Cu_3O_{6.48}$ is attributed predominately to a finite range of the structural order of the $x = 6.5$ phase, so that the NQR line width would be expected nearly identical among the various lattice sites. The experimental results shown in Fig.4(a), however, show that the line widths (in full width of half maximum) are dependent largely on sites; 0.4, 1.4, 1.4 and 1.5 MHz for 2-fold Cu(1), Cu(2A) and Cu(2B) and 4-fold Cu(1) sites, respectively. Since both 2-fold Cu(1) and the two Cu(2) sites have $\eta = 0$, the observed difference in line width means that the distribution of V_{zz} component is 3.5 times larger for Cu(2) plane sites than 2-fold Cu(1) chain sites. This discrepancy between the simple conjecture and the experimental result can be resolved easily by taking account of the antishielding effect. The contribution of lattice ions to the EFG at a site is enhanced by a factor of $1 - \gamma_\infty$ due to the antishielding effect of the ion itself. It is found from Tab.I that Cu^{2+} ions are 3.3 times larger in the antishielding factor compared with Cu^{1+} ions. This ratio is in good agreement with that of the observed NQR line widths (3.5 times). Therefore we can simply say that the ratio of NQR line widths observed at different sites is governed in the present system by the ratio of antishielding factors of the ions.

§8. Concluding Remarks

The values of $\langle r^{-3} \rangle$ have been obtained from the analysis of the copper quadrupole interaction for both the superconducting phase and the insulating one. The values are found to be not so much changed between the two phases, and yet to remain lying within the range expected for a Cu^{2+} ion in insulators.

We have also investigated in detail the hyperfine interaction at Cu(2) plane sites in $YBa_2Cu_3O_x$ system ($6.0 \leq x \leq 6.98$). The $K - \chi$ plot analysis has been made, for the first time, for the Cu NMR in the high T_c oxide and CuO. The anisotropic part of the hyperfine interaction can be described in terms of a usual Cu^{2+} ionic model, whereas the model fails to account for the isotropic (Fermi contact) part over the entire range of x. The present Cu NMR results suggest that, in addition to a usual core polarization hf, another, large and positive, contribution to the Fermi contact hf is required to produce the observed values of hfs in $YBa_2Cu_3O_x$ system. Such an anomalous hf is not present in CuO. Although we can not determine, within the experimental errors and the approximations involved in the present analysis, whether or not the magnitude of the anomalous hf is dependent on the oxygen concentration x, it is sure that a similar anomalous hf should be present in the insulating phase $x = 6.0$ as well. Therefore, the anomalous hf is unlikely to originate from the doped holes (carriers). It is shown that the origin is most likely the supertransferred hyperfine interaction arising from a covalent electron transfer through the linear bonds Cu^{2+}—O^{2-}—Cu^{2+}. This mechanism can reasonably be expected to be sensitive both to the bridging angle of the bonds and to the charge transfer gap (Δ). In view of these factors, we can find that the perovskite type structure is favorable to the supertransferred mechanism than a structure of edge-sharing net-work appearing in CuO.

Interestingly, it can be shown that the essential feature extracted in the present NMR study for $YBa_2Cu_3O_x$ system is common to the other high T_c copper oxides. As can be seen in Fig.12(d) and (e) and Fig.13(c) and (d), the sum $A_{cp} + A^{\perp}_{dip} + A^{\perp}_{so}$ amounts to a small value, because these components are approximately canceled with each other. If $A_{tr} = 0$, then we can expect,

$$|A_{AF}^{\perp}| = |A^{\perp}| = |A_{cp} + A_{dip}^{\perp} + A_{so}^{\perp}| \approx 0\,, \quad (17)$$

as has been observed in CuO. On the contrary, in the case of $YBa_2Cu_3O_{6.0}$, most of the observed internal hf $A_{AF}^{\perp} = H_n/\langle S\rangle$ is found to be attributed to the anomalous hf A_{tr} as can be seen in Fig.13(e). Therefore we can, in general, make a rough estimation of the value of A_{tr} by the measurement of the internal hf $A_{AF}^{\perp}$. In fact, we have observed Cu NMR in various antiferromagnetic copper oxides, such as La_2CuO_4 (Tsuda *et al.*, 1988), Nd_2CuO_4 (Yoshinari *et al.*, 1989), $Pb_2Sr_2YCu_3O_8$ (Yoshimura *et al.*, 1989). The zero field NMR spectra taken at $T = 4.2$ K have shown that the internal hfs in these oxides all lie within the region of $\pm(80 - 100)$ kOe and the ordered moments are oriented in the c-plane. These data clearly indicate that the anomalous hf A_{tr} should be present in these oxides as well as in $YBa_2Cu_3O_{6.0}$. All these oxides show the layered perovskite type structure and superconductivities by doping holes. Thus, we can evolve the outstanding feature common to the high T_c copper oxides that the type of charge and spin fluctuations which appear in process A are important.

The spin fluctuations can be probed by the measurements of the nuclear spin-lattice (T_1) and the spin-spin (T_2) relaxation times, as have been reported by, for example, Yasuoka *et al.*(1989) and Pennington *et al.*(1989a). In spite of considerable efforts of the experimental and theoretical studies on the relaxation times, we are still far from the full explanation. One of the difficulties stem from the importance of the degrees of freedom of the ligand electrons. This importance results from an interplay of the smallness of the charge transfer gap Δ and the geometry of the $\phi = 180°$ bonds. In the previous picture which has been used to interpret the magnetism and the superconductivity in transition metal compounds, only the d-states have often been considered. We have to study how to incorporate the degrees of freedom of the ligand electrons with the copper d-states.

Acknowledgments

We would like to thank K. Kosuge, K. Yoshimura, K. Okuda, H. Takagi, Y. Tokura, K. Kishio and K. Kitazawa for their material syntheses. We are indebted to K. Terakura, Y. Takahasi, H. Alloul and C. P. Slichter for fruitful discussions of this analysis.

References

Abragam A. and Bleaney, B., 1970, in *Electron Paramagnetic Resonance* Clarendon press, Oxford.
Adrian, F., J., 1988, Phys. Rev. B **38**, 2426.
Alloul, H., Ohno, T. and Mendels, P., 1989, Phys. Rev. Lett. **63**, 1700.
Annett, J. F., Goldenfeld N. and Renn, S. R. preprint.
Åsbrink, S and Norrby, L. J, 1970, Acta Cryst. **26**, 8.
Barrett, S. E., Durand, D. J., Pennington, C. H., Slichter, C. P., Friedmann, T. A., Rice, J. P., and Ginsberg, D. M., 1989, to be published in Phys. Rev. B.
Bednorz ,J. G. and Müller, K. A., 1986, Z. Phys. B **64**, 189.
Bianconi, A., Castellano, A. C., De Santis, M., Rudolf, P., Lagarde, P., Flank, A. M. and Marcelli, A., 1987, Solid State Commun. **63**, 1009.
Cava, R. J., *et al.*, 1988, Physica **C153-155**, 560.
Coffman, R., 1968, J. Chem. Phys. **48**, 609.
Farrel, D. E., 1987, *et al.*, Phys. Rev. B **36**, 4025.
Forsyth, J. B., Brown, P. J. and Wanklyn, B. M., 1988, J. Phys. C **21**, 2917.
Freeman, A. J. and Watson, R. E., 1965, in *Magnetism IIA* Academic press.
Fujimori, A. and Minami, F., 1984, Phys. Rev. B **30**, 987.
Fujimori, A., Takayama-Muromachi, E. and Uchida, Y., 1987a, Solid State Commun. **63**, 857.
Fujimori, A., Takayama-Muromachi, E., Uchida, Y. and Okai, B.,1987b, Phys. Rev. B **35**, 8814.
Hammel, P. C., Takigawa, M., Heffner, R. H. and Fisk, Z., 1988, Phys. Rev. B **38**, 2832.
Hay, P. J., Thibeault, J. C. and Hoffmann, R., 1975, J. Am. Chem. Soc. **97**, 4884.
Horvatić, M., Segransan, P., Berthier, C., Berthier, Y., Butaud, P., Henry, J. Y., Couach, M., Chaminade, J. P., 1989a, Phys. Rev. B **39**, 7332.
Horvatić, M., Segransan, P., Berthier, Y., Butaud, P., Kitaoka, Y., Berthier, C., Henry, J. Y. and Couach, M., 1989b, procedings of International M^2S-HTSC Conference, Stanford, Physica C.
Huang, N. L., Orbach, R., Šimáneki, E.,Owen, J. and Taylor, D. R., 1967, Phys. Rev. **156**, 383.
Hüfner, S., 1985, Z. Phys. B **61**, 135.
Itoh, M., Karashima, K., Kyogoku, M. and Aoki, I. 1989, Physica **C160**, 177.
Jeffrey, K. R. and Armstrong, R. L., 1966, Can. J. Phys. **44** 2315. Johnston, D. C., 1989, Phys. Rev. Lett. **62**, 957.
Johnston, D. C., Sinha, S. K., Jacobson, A. J. and Newsam, J. M., 1988, Physica **C153-155**, 572.
Junod, A. *et al.*, 1989 procedings of International M^2S-HTSC Conference, Stanford, Physica C.
Kamimura, H., 1966, J. Phys. Soc. Japan. **21**, 484.
Kanoda, K., Kawagoe,T., Hasumi, M., Takahashi, T., Kagoshima, S. and Mizoguchi, T., 1988, J. Phys. Soc. Japan. **57**, 1554.
Kawagoe, T., Mizoguchi, T., Kanoda, K., Takahashi, T., Hasumi, M. and Kagoshima, S., 1988, J. Phys. Soc. Japan. **57**, 2272.
Kheinmaa, I. A., Vainrub, A. M., Past, Ya, O., Miidel, V. A., Miller, A. V., Shchegolev, I. F., Emelchenko, G. A. and Tatarchenko, V. A., 1988, JETP Lett. **48**, 186.
Kitaoka, Y., Berthier, Y., Butaud, P., Horvatić, M., Ségransan, P., Berthier, C., Katayama-Yoshida, H., Okabe, Y. and Takahashi, T., 1989 procedings of International M^2S-HTSC Conference, Stanford, Physica C.
Kohori,Y., Shibai, H., Oda, Y, Kohara, T., Kitaoka, Y. and Asayama, K., 1988, J. Phys. Soc. Japan. **57**, 744.
Locher, P. R. and Van Stapele, R. P., 1970, J. Phys. Chem. Solid **31**, 2643.
Lütgemeier, H., 1988, Physica **C153-155**, 95.
Mali, M., Brinkman, D., Pauli, L., Roos, J., Zimmermann, H. and Hulliger, J., 1987, Phys. Lett. A **124**, 112.
Mendels, P. and Alloul, H., 1988, Physica **C156**, 355.
Mila, F. and Rice, T. M., 1989, Physica **C157**, 561.
Nakazawa Y. and Ishikawa, M., 1989, Physica **C158**, 381.
Nücker, N., Fink, J., Fuggle, J. C., Durham, P. J. and Temmerman, W. M., 1988, Phys. Rev. B **37**, 5158.
Oguchi, T., Park, K. E., Terakura, K. and Yanase, A., 1987, Physica **148B**, 253-256
Oldfield, E., Coretsopoulos, C., Yang, S., Reve, L., Lee, H. C., Shore, J., Han, O. H., Ramli, E. and Hinks, D., 1989, Phys. Rev. B **40**, 6832.
Park, K. E., Terakura, K., Oguchi, T., Yanase, A. and Ikeda, M., 1988, J. Phys. Soc. Japan. **57**, 3445.
Parkin, S. S. P., Engler, E. M., Lee, V. Y. and Beyers, R. B., 1988, Phys. Rev. B **37**, 131.
Pauling, L., 1987, Phys. Rev. Lett. **59**, 225.
Pennington, C. H., Durand, D. J., Zax, D. B., Slichter, C. P., Rice, J. P. and Ginsberg, D. M., 1988, Phys. Rev. B **37**, 7944.
Pennington, C. H., Durand, D. J., Slichter, C. P., Rice, J. P., Bukowski, E. D. and Ginsberg, D. M., 1989a, Phys. Rev. B **39**, 274.

Pennington, C. H., Durand, D. J., Slichter, C. P., Rice, J. P., Bukowski, E. D. and Ginsberg, D. M., 1989b, Phys. Rev. B **39**, 2902.

Pickett, W. E., 1989, Rev. Mod. Phys. **61**, 439.

Shen, Z., Allen, J. W. , Yeh, J. J., Kang, J. -S., Ellis, W., Spicer, W., Lindau, I. Maple, M. B., Dalichaouch, Y. D., Torikachvili, M. S., Sun, J. Z. and Geballe, T. H., 1987, Phys. Rev. B **36**, 8414.

Shimizu, T., Yasuoka, H., Imai, T., Tsuda, T., Takabatake, T., Nakazawa, Y. and Ishikawa, M., 1988, J. Phys. Soc. Japan. **57**, 2494.

Šimánek, E. and Müller, K. A., 1970, J. Phys. Chem. Solids, **31**, 1027-1040.

Šimánek, E. and Šroubek, Z., 1972, in *Electron Paramagnetic Resonance*, edited by Geschwind, S., (Plenum Press).

Takigawa, M., Hammel, P. C., Heffner, R. H., Fisk, Z., Smith, J. L.and Schwarz, R. B., 1989a, Phys. Rev. B **39**, 300.

Takigawa, M., Hammel, P. C., Heffner, R. H. and Fisk, Z., 1989b, Phys. Rev. B **39**, 7371.

Takigawa, M., Hammel, P. C., Heffner, R. H., Fisk, Z., Ott, K. C.and Thompson, J. D., 1989c, Phys. Rev. Lett. **63**, 1865.

Taylor, D. R., Owen, J., and Wanklyn, Barabara, M., 1973, J. Phys. C **6**, 2592.

Ting, Y. and Lew, H., 1957, Phys. Rev. **105**, 581.

Tranquada, J. M., Moudden, A. H., Goldman, A. I., Zolliker, P., Cox, D. E., Shirane, G., Sinha, S.K., Vaknin, D., Johnston, D. C., Alvares, M. S., Jacobson, A. J., Lewandowski, J. T. and Newsam, J. M., 1988, Phys. Rev. B **38**, 2477.

Tsuda, T., Shimizu, T., Yasuoka, H., Kishio, K. and Kitazawa, K., 1988 , J. Phys. Soc. Japan. **57**, 2908. There is an erratum in this paper. The value of the internal field 78.78 kOe in La_2CuO_4 should be replaced by 81.87 kOe, although the Larmor frequency is correct.

Ueda, Y. and Kosuge, K., 1988, Physica C **156**, 281.

Walstedt, R. E., Warren, W. W. Jr., Tycko, R., Bell, R. F., Brennert, G. F., Cava, R. J., Schneemeyer, L. and Waszczak, J., 1988, Phys. Rev. B **38**, 9294.

Watson, R. E. and Freeman, A. J., 1961, Phys. Rev. **123**, 2027.

Willett, R. D. and Landee, C. P.,1981, J. Appl. Phys. **52**, 2004.

Yamaguchi, Y., Tokumoto, M., Waki, S., Nakagawa, Y. and Kimura, Y., 1989, J. Phys. Soc. Japan. **58**, 2256.

Yasuoka, H, Shimizu, T, Ueda Y. and Kosuge, K., 1988, J. Phys. Soc. Japan. **57**, 2659. There is an erratum in this paper. The value of the internal field 76.65 kOe in $YBa_2Cu_3O_6$ should be replaced by 79.65 kOe, although the Larmor frequency is correct.

Yasuoka, H., Shimizu, T., Imai, T., Sasaki, S., Ueda, Y. and Kosuge, K., 1989, in Proceedings of the International Conference on Nuclear Methods in Magnetism, Münich, 49, 167.

Yasuoka, H., Imai, .T., and Shimizu, T., 1989, to be published in "Strong Correlation and Superconductivity", eds., Fukuyama, H., Maekawa, S., and Morozemoff, A. P. (Spring-Verlag. Berlin, 1989).

Yoshimura, K. *et al.*, 1989, to be submitted to J. Phys. Soc. Jpn.

Yoshinari, Y., Yasuoka, H., Shimizu, T., Takagi, H., Tokura, Y. and Uchida S., 1989, in press, J. Phys. Soc. Jpn. **59**, No. 1.

Zaanen, J. and Sawatzky, G. A., 1987, Can. J. Phys. **65**, 1262.